

# UC San Diego

## UC San Diego Previously Published Works

### Title

Targeting colorectal cancer via its microenvironment by inhibiting IGF-1 receptor-insulin receptor substrate and STAT3 signaling.

### Permalink

<https://escholarship.org/uc/item/2k10p4b5>

### Journal

Oncogene, 35(20)

### ISSN

0950-9232

### Authors

Sanchez-Lopez, E  
Flashner-Abramson, E  
Shalapour, S  
et al.

### Publication Date

2016-05-01

### DOI

10.1038/onc.2015.326

Peer reviewed



Published in final edited form as:

*Oncogene*. 2016 May 19; 35(20): 2634–2644. doi:10.1038/onc.2015.326.

## Targeting colorectal cancer via its microenvironment by inhibiting IGF-1 Receptor-insulin receptor substrate and STAT3 signaling

Elsa Sanchez-Lopez<sup>1</sup>, Efrat Flashner-Abramson<sup>2</sup>, Shabnam Shalpour<sup>1</sup>, Zhenyu Zhong<sup>1</sup>, Koji Taniguchi<sup>1,3</sup>, Alexander Levitzki<sup>2</sup>, and Michael Karin<sup>1</sup>

<sup>1</sup>Laboratory of Gene Regulation and Signal Transduction, Departments of Pharmacology and Pathology, School of Medicine, University of California, San Diego, 9500 Gilman Drive, La Jolla, CA, 92093-0723, USA

<sup>2</sup>Unit of Cellular Signaling, Department of Biological Chemistry, The Alexander Silberman Institute of Life Sciences, The Hebrew University of Jerusalem, Jerusalem, Israel

<sup>3</sup>Department of Microbiology and Immunology, Keio University School of Medicine, 35 Shinanomachi, Shinjuku-ku, Tokyo 160-8582, Japan

### Abstract

The tumor microenvironment (TME) exerts critical pro-tumorigenic effects through cytokines and growth factors that support cancer cell proliferation, survival, motility and invasion. Insulin-like growth factor-1 (IGF-1) and Signal transducer and activator of transcription 3 (STAT3) stimulate colorectal cancer (CRC) development and progression via cell autonomous and microenvironmental effects. Using a unique inhibitor, NT157, which targets both IGF-1 receptor (IGF-1R) and STAT3, we show that these pathways regulate many TME functions associated with sporadic colonic tumorigenesis in CPC-APC mice, in which cancer development is driven by loss of the *Apc* tumor suppressor gene. NT157 causes a substantial reduction in tumor burden by affecting cancer cells, cancer-associated fibroblasts (CAF) and myeloid cells. Decreased cancer cell proliferation and increased apoptosis were accompanied by inhibition of CAF activation and decreased inflammation. Furthermore, NT157 inhibited expression of pro-tumorigenic cytokines, chemokines and growth factors, including IL-6, IL-11 and IL-23 as well as CCL2, CCL5, CXCL7, CXCL5, ICAM1 and TGF $\beta$ ; decreased cancer cell migratory activity and reduced their proliferation in the liver. NT157 represents a new class of anti-cancer drugs that affect both the malignant cell and its supportive microenvironment.

Users may view, print, copy, and download text and data-mine the content in such documents, for the purposes of academic research, subject always to the full Conditions of use: [http://www.nature.com/authors/editorial\\_policies/license.html#terms](http://www.nature.com/authors/editorial_policies/license.html#terms)

Corresponding Author: Professor Michael Karin, Laboratory of Gene Regulation and Signal Transduction, Departments of Pharmacology and Pathology, School of Medicine, University of California, San Diego. 9500 Gilman Drive, La Jolla, CA, 92093-0723, USA, ; Email: [karinoffice@ucsd.edu](mailto:karinoffice@ucsd.edu), Phone

**Conflict of interest:** The authors declare no conflict of interest.

Supplementary Information accompanies the paper on the *Oncogene* website (<http://www.nature.com/onc>).

## Keywords

IGF-1R; IRS1/2; STAT3; Colorectal cancer; Tumor Microenvironment

## INTRODUCTION

Colorectal cancer (CRC) is the third most commonly diagnosed cancer, with approximately 1.2 million new cases each year. Improved early detection and patient stratification have resulted in a significant reduction of mortality, but most of the improvement has been limited to early stage CRC (stages I and II), and in patients with advanced stage III and IV disease, morbidity and mortality remain high<sup>1</sup>. CRC originates from epithelial cells at the base of intestinal crypts, which accumulate activating oncogenic mutations with concomitant loss of tumor suppressor genes, especially *APC*<sup>2</sup>. About 2–3% of all CRC cases are associated with pre-existing inflammation and are referred to as colitis associated cancer, or CAC<sup>3</sup>, whose development is highly dependent on NF- $\kappa$ B signaling in tumor-associated macrophages (TAM), which leads to indirect activation of STAT3 in pre-malignant intestinal epithelial cells (IEC)<sup>4,5</sup>.

STAT3, a crucial and well-known mediator of malignant progression in CRC<sup>5,6</sup>, is predominantly activated by IL-6<sup>5</sup> and IL-11<sup>7</sup>. Immune cells and cancer-associated fibroblasts (CAF) within the TME actively contribute to sustained STAT3 activation in CRC. Secretion of IL-11 by TGF- $\beta$ -stimulated CAF triggers STAT3 signaling in cancer cells<sup>8</sup>, and IL-6 produced by TAM protects normal and premalignant IEC from apoptosis also through STAT3 activation<sup>5</sup>. Moreover, activation of IL-6-STAT3 signaling in normal gastric fibroblasts contributes to their conversion into CAF<sup>9</sup>. Such findings indicate that tumor development is highly dependent on intricate interactions between multiple cell types, in addition to malignant epithelial cells that harbor oncogenic mutations<sup>3,10,11</sup>. We found that inflammatory processes also play a critical role in development of sporadic CRC, which is driven by *APC* loss<sup>12</sup>. Absence of APC in IEC results in rapid loss of several components of the epithelial barrier that prevent invasion of the colonic mucosa by components of the endogenous microbiome, thereby leading to highly elevated expression of the key inflammatory cytokine IL-23 in myeloid cells<sup>12</sup>. By expanding the number of IL-17-producing cells, IL-23 provides a supportive inflammatory microenvironment that accelerates tumor progression<sup>12,13</sup>.

The TME, which is enriched in immune cells including TAM and various lymphocytes, as well as CAF, can also affect the response to therapy in many cancers, including CRC<sup>14,15</sup>. Anticancer drugs are frequently rendered ineffective against cancer cells that are co-cultured with stromal cells<sup>16</sup>. For this reason, identification of therapeutic targets that concomitantly affect the malignant behavior of cancer cells and the supportive function of the TME is of particular importance. Although targeted biological therapy is rapidly becoming the standard of care in advanced CRC<sup>17</sup>, very few targeted therapeutics were found to affect the TME. Of note, antagonists of epidermal growth factor receptor (EGFR) mainly affect malignant epithelial cells, but inhibitors of vascular endothelial growth factor (VEGF) target the TME and block its ability to stimulate tumor angiogenesis but have no direct activity on cancer

cells<sup>17</sup>. Therefore, EGFR and VEGF inhibitors need to be combined, in order to target both the malignant cell and its supportive microenvironment.

In addition to STAT3, another potential therapeutic target in CRC is the ubiquitously expressed insulin-like growth factor 1 receptor (IGF-1R), which is involved in diverse processes, including mitogenesis, cell survival and differentiation<sup>18,19</sup>. *In vitro* experiments and epidemiological studies have suggested that IGF-1R participates in the pathogenesis of many neoplastic diseases, including CRC<sup>19,21</sup>. Elevated IGF-1R and IGF-1 expression correlates with tumor progression and poor prognosis in several cancer types including gastrointestinal malignancies<sup>21,22</sup>. Genetic polymorphisms in genes encoding IGF-1R signaling components and increased circulating IGF-1 or IGF-2 were detected in CRC patients<sup>23,25</sup>. In addition, IGF-1R-driven PI3K/AKT signaling, predicts poor survival in CRC independently of the *KRAS* mutational status<sup>25</sup>. Furthermore, IGF-1R signaling contributes to resistance to cytotoxic<sup>26</sup>, radiation<sup>27</sup> and targeted<sup>28,30</sup> therapies. Importantly, the pro-oncogenic activities of IGF-1R are highly dependent on its proximal downstream effectors: insulin receptor substrate 1 (IRS1), and IRS2<sup>31,32</sup>. IRS1 is upregulated in primary and metastatic human CRC compared to the normal colonic epithelium<sup>33</sup>. *Apc*<sup>MIN</sup> mice, which carry an inactivating somatic mutation in the murine *Apc* gene, develop significantly fewer intestinal adenomatous polyps when the *Irs1* gene is inactivated<sup>32</sup>.

The involvement of IRS proteins in tumor progression, metastasis and acquired drug resistance<sup>31,34,35</sup> establishes them as potential and novel targets for anti-cancer drugs. With that in mind, NT157 was developed as a prototypic, first-in-class, compound that binds to an allosteric site on IGF-1R and induces a conformational change, which results in dissociation of receptor-bound IRS1 and IRS2 proteins<sup>35</sup>. This allows IGF-1R to interact more strongly with the adaptor protein Shc, resulting in enhanced activation of ERK, which mediates serine phosphorylation and subsequent proteolysis of IRS proteins. Eventually, NT157 leads to long-lasting IGF-1R inhibition, cancer cell apoptosis and additional antitumor effects, independently of IGF-1 binding<sup>35</sup>. Another IGF-1R-independent effect of NT157 is the dephosphorylation of STAT3 (see accompanying manuscript). The ability of NT157 to inhibit two different signaling pathways critical for CRC development drove us to test its activity in both sporadic and metastatic CRC mouse models. We now show that NT157 prevents colorectal tumor development, leads to durable regression of established tumors and attenuates growth in the liver metastatic niche. In addition to having direct effects on cancer cells, NT157 inhibits critical components of the TME, including CAF and TAM. Thus, NT157 is a new type of therapeutic compound that, as a single agent, concomitantly targets two essential signaling pathways in malignant cells and components of their supportive microenvironment, resulting in strong and pluripotent anti-cancer activity.

## RESULTS

### NT157 reduces tumor burden in CPC-APC mice

We used a mouse model of sporadic colorectal tumorigenesis, the CPC-APC mouse, in which one *Apc* tumor suppressor allele is specifically deleted in the distal colonic epithelium and the second allele undergoes loss-of-heterozygosity (LOH), the same process that drives human CRC development<sup>36</sup>. APC-deficient intestinal organoids exhibited elevated IGF-1R

and IRS1 mRNA expression, whereas colonic tumors from CPC-APC mice showed elevated expression of IGF-1R, IRS1 and IRS2 mRNAs (Supplementary Figure 1A,B). IGF-1R was widely expressed in several TME cell types, including epithelial cancer cells, CAF and myeloid cells (Supplementary Figure 1C). Elevated IGF-1 in the circulation and in tumor-CM was also observed (Supplementary Figure 1D,E). Consistent with previous results<sup>35</sup>, treatment of APC-deficient intestinal organoids and tumor-bearing mice with NT157 resulted in a rather rapid decrease in IRS1 abundance (Supplementary Figure 1F-H). Encouraged by these results, we subjected CPC-APC mice, which develop colonic adenomas at 8 to 10 weeks of age, to either early (initiated at 8 weeks) or late (initiated at 16 weeks) treatment with NT157 (Figure 1a). In both cases, NT157 treatment significantly reduced tumor burden (Figure 1b,c), suggesting a role for the IGF-1R-IRS axis in colonic tumor development and maintenance in CPC-APC mice. Kaplan-Meier analysis of the late treatment group confirmed that NT157 used as a single agent significantly prolonged survival (Figure 1d). Even 7 weeks after treatment termination, tumor size remained significantly suppressed in NT157 treated mice (Supplementary Figure 1I). NT157 treatment reduced the proliferation and induced apoptosis of cancer cells (Figure 1e,f), along with IRS1 Ser-phosphorylation (Figure 1g).

### NT157 reduces tumor inflammation and reactive stroma

The IGF-1R-IRS and the IL-6-STAT3 signaling pathways are co-activated in different pathological contexts<sup>37,38,39</sup>. NT157 treatment inhibited STAT3 activation in several cancer cells lines (see accompanying manuscript), including murine and human CRC cells and the TME (Figure 2a, b, d). NT157 slightly increased SHP2 protein expression in some cell lines, but that did not correlate with its effects on STAT3 activation by IL-6, which was consistently inhibited (Figure 2c, d). STAT3 stimulates *Cox2* gene transcription<sup>40</sup> and correspondingly NT157 blocked COX-2 expression in the TME (Figure 2a,b). NT157 treatment also reduced the expression of numerous chemokines, chemokine receptors and proinflammatory cytokines, including CCL2, CCR2, CCL5, IL-6, IL-11, IL-22 and IL-23 (Figure 2e), which was accompanied by a decrease in intratumoral CD11b<sup>+</sup> and F4/80<sup>+</sup> cells, and  $\alpha$ SMA-expressing CAF (Figure 2f). Reduced CAF activation was associated with decreased collagen type I deposition and fibrogenic genes expression (Supplementary Figure 2A,B).

### NT157 inhibits cancer cell proliferation and signaling

To better understand the cellular targets for NT157, we evaluated which effects are rapidly induced by NT157 and which are the consequence of prolonged treatment. We treated 16 week-old CPC-APC mice with NT157 for one week, and sacrificed them 24 hrs after the last dose. Even this short treatment period decreased tumor multiplicity (Figure 2g). After only two doses, NT157 reduced the number of proliferative Ki67<sup>+</sup> cells in tumors, and induced cancer cell death, without affecting the normal tissue (Figure 2h,i). We further evaluated the effect of NT157 on TME populations. After short NT157 treatment, no changes in immune cell populations in spleen, mesenteric lymph nodes (MLN) and normal colon tissue were observed (Supplementary Figure 3A,B). No significant changes in tumoral myeloid-derived suppressor cells (CD11b<sup>+</sup>Gr-1<sup>+</sup>), dendritic cells (CD11b<sup>+</sup>MHCII<sup>+</sup>CD11c<sup>+</sup>), inflammatory macrophages (CD11b<sup>+</sup>MHCII<sup>+</sup>F4/80<sup>+</sup>), or lymphocytes (CD4<sup>+</sup>, CD8<sup>+</sup>, NK1.1<sup>+</sup> and CD19<sup>+</sup>)

were found, either (Supplementary Figure 3C,D). Also, no changes in ROR $\gamma$ <sup>+</sup> or IL-17A-producing cells in MLN and spleen were observed (Supplementary Figure 3F), neither was expression of Th17 signature genes, other than IL-21 (Supplementary Figure 3G). By contrast, a substantial reduction in gp38<sup>+</sup> $\alpha$ SMA<sup>+</sup> CAF abundance was observed (Supplementary Figure 3E), suggesting that inhibition of CAF activation represents a rapid response to NT157 treatment.

Consistent with its ability to induce IRS1 degradation, NT157 led to ERK1/2 activation independently of IGF-1 (Figure 3a,b,d and Supplementary Figure 4H). This was accompanied by inhibition of the PI3K-AKT-mTOR pathway, as indicated by reduced phosphorylation of AKT, ribosomal protein S6 and 4E-BP, especially upon IGF-1 stimulation (Figure 3a–d and Supplementary Figure 4H). The anti-proliferative effect of NT157 in mouse and human CRC cell was reflected in reduced cell viability (Supplementary Figure 4A–F) and cyclin D1 expression, and caspase-3 activation at 48 hrs after treatment initiation. In APC-deficient organoids, NT157 also inhibited cyclin D1 expression (Figure 3f). These results indicate that disruption of the IGF-1R-IRS axis inhibits downstream signaling pathways that control cancer cell proliferation and survival. A further decrease in cell survival and proliferation is likely to be caused by inhibition of STAT3 activation.

### NT157 decreases CRC cell growth in the metastatic niche

IGF-1R signaling and IRS proteins control migratory and invasive behavior of cancer cells<sup>31,34</sup>. In the presence of IGF-1, the MC-38, HCT116 and DLD-1 cell lines displayed enhanced migratory behavior, as shown by scratch and boyden chamber assays, and this behavior was inhibited by NT157 (Figure 4a–d and Supplementary Figure 4I). Several chemokines produced by cancer cells may facilitate migratory behavior<sup>41,42</sup>. Of note, NT157 inhibited expression of CXCL5 and CXCL7 in MC-38 cells incubated with LPS, a TLR4 agonist (Supplementary Figure 5A). Although NT157 did not affect the expression of CCL20 or CXCL12 in MC-38 cells, it did reduce CCL2 expression (Supplementary Figure 5A). Long-term treatment with NT157 also decreased the expression of CXCL5, MIP-2 $\gamma$  and IL-8 in colonic tumors (Supplementary Figure 5B). To test the effect of NT157 on the metastatic growth of CRC cells in liver, we injected MC-38 cells intrasplenically and initiated treatment with NT157 one week later (Figure 4e). NT157 treatment significantly decreased the size of liver metastases (Figure 4f,g), and reduced cell proliferation within metastatic nodules (Figure 4h, i). Importantly, the number of  $\alpha$ SMA-expressing cells surrounding CRC cells in the liver was also diminished after NT157 treatment (Figure 4h, i). These data suggest that NT157 targets CRC cells that migrate, reducing their ability to grow at the new site and inhibiting the support they receive from activated myofibroblasts or hepatic stellate cells.

### NT157 inhibits CAF and macrophage activation

IGF-1 is a well-known autocrine and paracrine inducer of CAF activation<sup>15</sup>. We isolated CAF from CPC-APC mice, and stimulated them with IGF-1. This resulted in increased  $\alpha$ SMA expression, which was abolished when cells were treated with NT157 (Figure 5a,b). NT157 treatment also decreased the induction of collagen type I as well as TGF $\beta$ , CTGF and

FAP mRNAs (Figure 5b). Activated CAF also produced inflammatory cytokines, including IL-6 and IL-11, and matrix metalloproteinases<sup>15</sup>, including MMP3, which expression was also abolished by NT157 (Figure 5b). NT157 also inhibited induction of IL-6, IL-11, collagen type I, CTGF and TGF $\beta$  mRNAs by other CAF activators, including CTGF and TGF $\beta$  (Supplementary Figure 6a).

TAM are another important source of tumor-promoting cytokines in CRC<sup>3</sup>. Although we did not observe an obvious effect on the number of TAM after short term NT157 treatment, long term NT157 treatment reduced the expression of numerous inflammatory cytokines (Figure 2d). To test the effect of NT157 treatment on macrophages, we used bone marrow-derived macrophages (BMDM). Using LPS as a generic BMDM activator, we found that NT157 inhibited the induction of IL-6, IL-11 and IL-10 mRNAs (Figure 5c) and the, presumably autocrine, activation of STAT3 (Figure 5d). Consistent with these results, NT157 also inhibited the induction of IL-23, IL-12, IFN $\gamma$  and IL-1 $\beta$  mRNAs (Figure 5e). Surprisingly, NT157 enhanced the secretion TNF secretion, while inhibiting IL-6 secretion (Figure 5f).

## DISCUSSION

In addition to the genetic and epigenetic alterations that account for malignant transformation, the TME is another key regulator of tumorigenesis and metastatogenesis. In particular, inflammatory cell infiltration and activation in early stages of colorectal tumorigenesis enhances proliferation of transformed IEC in which  $\beta$ -catenin has been activated, and renders them resistant to apoptotic elimination<sup>3,10</sup>. This microenvironmental effect is responsible for accelerating of tumor progression. Deposition of extracellular matrix (ECM) by CAF further facilitates tumor growth and spread through effects on endothelial cells that turn on the angiogenic switch<sup>14,15</sup>. The emergence of the TME as an essential driver of malignant progression suggests that therapies that target TME components in addition to cancer cells, should have strong anti-tumor activity. Although TME-targeting therapies should be less susceptible to development of drug resistance because the TME is composed of genetically normal and stable cells, the existence of several distinct and interactive cell types within the TME, each relying on different signaling pathways, renders this task a difficult one. For instance, anti-angiogenic therapies that target VEGFR on endothelial cells were found to upregulate components of the EGFR and FGFR signaling pathways in the tumor bed<sup>43</sup>. Another unexpected effect is exhibited by anti-CCL2 therapy, which potentiates metastasis within weeks after its termination, by enhancing macrophage recruitment into metastatic sites<sup>44</sup>. Taking all of these points into consideration, we examined the ability of NT157, a novel tyrphostin that can inhibit at least two oncogenic signaling pathways, IGF-1R-IRS and JAK-STAT3, to target both carcinoma cells and their microenvironment in a mouse model of sporadic CRC. Our results demonstrate that NT157 effectively reduced tumor multiplicity and size through pleiotropic effects on CRC cells and the reactive stroma within which they reside. The rapid inactivation of CAF, and inhibition of cancer cell proliferation and viability, as well as cytokine production, result in a less reactive microenvironment and a further decrease in myeloid cell infiltration. Importantly, the inhibition of STAT3 and IGF-1R-IRS signaling by NT157 prolongs the survival of CPC-APC mice, in which CRC development is driven by the same genetic and immune mechanisms responsible for development of aggressive human CRC<sup>12</sup>. In fact, weeks after



treatment cessation, colonic tumors in NT157-treated CPC-APC mice remain smaller than those in non-treated mice, supporting the idea that conversion of the TME compartment to a less reactive and less inflamed state along with cancer cell targeting results in severe impairment of malignancy. Our results strongly support further clinical evaluation of NT157 and similar compounds in sporadic human CRC.

At this point, it is difficult to discern whether inhibition of STAT3 or blockade of IGF-1R-IRS signaling makes a more important contribution to the anti-neoplastic activity of NT157. A role for the IGF-1R-IRS axis in the pathogenesis of CRC is supported by human association studies. Genetic polymorphisms in genes encoding IGF family members and related proteins, including IGF-1 and IGF1R, are associated with CRC development<sup>24</sup>. Elevated plasma IGF-1 and IGF-1R downstream signaling have been linked to enhanced risk of colorectal neoplasia and poor survival<sup>21,23,25,45</sup>. Importantly, a prospective study of a cohort of 210 CRC patients showed that tumor size and depth of invasion significantly correlate with IGF-1 and IGF-1R expression<sup>23</sup>. To closely mimic sporadic human CRC, we have used the CPC-APC mouse model, as both depend on loss of the APC tumor suppressor. In addition, CPC-APC mice exhibit strong activation of the IL-23-IL-17 cytokine cascade<sup>12</sup>, which predicts rapid progression to metastatic disease in human CRC<sup>46</sup>. We found that loss of APC expression in intestinal organoids and colonic tumors results in upregulation of IGF-1R and IRS1 expression, findings that are similar to those made in human CRC. We also found that several TME constituents, including CAF and TAM, exhibit activation of IGF-1R-IRS signaling, which is likely to be sustained by circulating IGF-1, whose concentrations in CPC-APC mice are higher than in control littermates. Combined with overexpression of IGF-1R and IRS proteins in CRC cells, elevated IGF-1 secretion into the tumor bed results in a strong activation of this pathway. Altogether, these findings justify the use of the CPC-APC model for evaluating the therapeutic efficacy of IGF-1R-IRS signaling inhibitors.

NT157 was identified as an IGF-1R signaling inhibitor that acts through a novel mechanism: binding of NT157 to IGF-1R promotes the detachment of IRS proteins, thereby facilitating Shc recruitment and activation of ERK1/2, which eventually phosphorylate IRS proteins and induce their degradation<sup>35</sup>. We have confirmed that in both murine and human CRC cells, NT157 activated ERK1/2, independently of IGF-1 binding to IGF-1R, resulting in inhibition of AKT activation. We also found that NT157 effectively inhibited the phosphorylation of mTORC1 downstream targets, including ribosomal protein S6 and 4EBP1. These effects may contribute to the ability of NT157 to inhibit cancer cell proliferation and survival. Another mechanism through which NT157 can compromise cancer cell proliferation and survival is inhibition of STAT3 activation (see accompanying manuscript). We confirmed that NT157 inhibited STAT3 tyrosine phosphorylation not only in colorectal tumors, but also in IL-6 treated murine and human CRC cells and LPS-stimulated macrophages. Importantly, our previous work indicated that STAT3 activation plays a critical role in the pathogenesis of both CAC in mice treated with AOM+DSS<sup>5</sup> and sporadic colonic tumorigenesis in CPC-APC mice<sup>12</sup>. STAT3 is involved in both the survival and the proliferation of CRC cells<sup>10</sup> and part of the anti-proliferative effect of NT157 could be due to inhibition of cyclin D1 expression, which is induced by STAT3. NT157 treatment also inhibited the expression of COX-2, which is also encoded by a STAT3 target gene. COX-2 is responsible for production



of prostaglandin E2 (PGE<sub>2</sub>), which stimulates malignant progression by promoting the survival of CRC cells and increasing their motility<sup>47</sup>. PGE<sub>2</sub> can also enhance production of IL-23 by myeloid cells<sup>3</sup>, which further stimulates CRC progression through the IL-23-IL-17 cytokine cascade. Notably, selective COX-2 inhibitors reduce CRC incidence<sup>48</sup>, although they also exacerbate intestinal injury<sup>3</sup>, thereby limiting their utility. In contrast, inhibition of COX-2 expression in colonic tumors by NT157 treatment offers a more selective therapeutic option for blocking the production of pro-tumorigenic PGE<sub>2</sub> in CRC.

Both CAF and myeloid cells contribute to STAT3 activation in cancer cells by producing IL-6 and IL-11<sup>12,15</sup>. Importantly, the anti-inflammatory and anti-tumorigenic effects of NT157 are also manifested in these major TME constituents. TAM are important regulators of solid tumor development based on their ability to enhance angiogenic, invasive and metastatic programming of neoplastic tissue, and their presence in human cancer usually correlates with a worse clinical outcome<sup>49</sup>. In BMDM stimulated with LPS, NT157 blocked the induction of IL-6, IL-11 and IL-10, pro-tumorigenic cytokines that mediate STAT3 activation, as well as IL-23, IL-12, IFN $\gamma$  and IL-1 $\beta$ . Surprisingly, however, NT157 enhanced TNF secretion in the presence of LPS, while inhibiting IL-6 secretion. The mechanistic basis for this phenomenon is far from clear, but it should be noted that no increase in intratumoral TNF was observed in NT157-treated CPC-APC mice. Importantly, NT157 treatment also decreased expression of several chemokines and chemokine receptors, including CCL2, CCR2 and CCL5 both in isolated cells and in tumors. This effect may explain the reduced amount of inflammatory infiltrate in colonic tumors of NT157-treated mice. However, NT157 did not affect intratumoral Th17 cells or their product, IL-17A. Nonetheless, inhibition of colonic tumor growth by NT157 was as extensive as the inhibition afforded by IL-17A neutralization, but unlike IL-17A neutralization, which only reduced tumor development when applied early<sup>13</sup>, the tumoricidal effect of NT157 was observed even when its administration was delayed until after tumor establishment. Furthermore, the therapeutic effect of NT157 was durable and was sustained for at least 7 weeks after treatment cessation and prolonged survival.

As cancers progress, their stroma becomes more reactive, phenotypically mimicking tissues undergoing wound healing or chronic inflammation. Indeed, many solid human malignancies are characterized by desmoplasia, containing high numbers of myofibroblasts<sup>15</sup>. CAF inactivation by NT157 was accompanied by decreased collagen type I expression and deposition, and reduced expression of fibrogenic and inflammatory cytokines, including CTGF, TGF $\beta$ , IL-6 and IL-11. In addition to eliminating the tumor supportive functions of the TME, NT157 treatment may also result in improved delivery of cytotoxic drugs. Importantly, the effects of NT157 are not limited to the TME and are also exerted on malignant epithelial cells. In addition to the inhibitory effects on cell proliferation and survival, NT157 also attenuates the migratory and invasive behavior of metastatic CRC cells and decreases their ability to proliferate forming metastatic lesions in the liver, the most common site of CRC metastasis. Although the precise mechanism by which NT157 inhibits liver metastasis remains to be determined, previous studies have revealed an important role for IL-6 signaling in this process<sup>50</sup>. Thus, it is conceivable that the effect of NT157 may be related to its ability to inhibit IL-6-induced STAT3 activation.

In summary, NT157 represents a new type of a multi-pronged therapeutic agent that targets at least two major oncogenic signaling pathways (IGF-1R-IRS and JAK-STAT3). Importantly, NT157 exerts its effects on several cell types involved in cancer development and progression, including malignant epithelial cells, CAF and TAM. This broad and pluripotent effect may explain the remarkable anti-tumor activity exhibited by NT157 when it was used as a single agent.

## METHODS

### Cell culture and reagents

HCT-116, SW620, HT29, SW480, DLD-1 cells were obtained from American Type Culture Collection (ATCC, Manassas VA, USA), and MC-38 cells from Dr. Shoshana Yakar. Cells were maintained in DMEM or RPMI with 10% FBS and 1% penicillin/streptomycin at 37°C and 5% CO<sub>2</sub>. CAF were isolated as described<sup>13</sup>. BMDM were derived from bone marrow and induced to differentiate with M-CSF for 7 days. Organoid cultures of small intestinal crypts were established as described<sup>13</sup>.

NT157 was synthesized by Dr. Salim Joubran from the Jerusalem laboratory and used as described<sup>35</sup>. LPS and IGF-1 were purchased from Sigma-Aldrich (St. Louis, MO, USA); and IL-6 from Goldbio (St. Louis, MO, USA).

### Mouse models of CRC

C57BL/6 mice were obtained from Charles River Laboratories. *Apc<sup>F/F</sup>*, *CDX2-Cre* (CPC-APC) mice were described<sup>36</sup>. Spontaneous colonic tumorigenesis was analyzed at 17 weeks of age, in the case of short-term treatment, or at 20 weeks of age, for late treatment. NT157 was i.p. injected at 70 mg/kg (in 20% 2-hydroxypropyl- $\beta$ -cyclodextrin) (Sigma-Aldrich), three times a week, until sacrifice. For survival analysis, mice were followed until moribund.

CRC metastasis to liver was studied by intrasplenic injection of  $5 \times 10^5$  MC-38 cells into 12 weeks old C57BL/6 females. Animals were sacrificed 20 days after cell injection.

All animal studies were performed in accordance with UCSD and NIH guidelines and regulations for the housing and treatment of laboratory animals.

### Protein Immunoblotting

Cells were lysed in NP40 buffer and analyzed by standard immunoblotting protocols. Antibodies used were directed against: ERK1/2, phospho-ERK1/2, phospho-STAT3, phospho-Akt S473, IRS1, phospho-IRS1 S636/639, IGF-1R, phospho-S6 ribosomal protein, phospho-4E-BP1, cyclin D1, cleaved caspase 3 (Cell Signaling, Danvers, MA, USA);  $\beta$ -catenin, SHP2, IRS1, GAPDH (Santa Cruz Biotechnology, Dallas, TX, USA); and  $\alpha$ -tubulin (Sigma-Aldrich). Secondary antibodies were from Cell Signaling. Detection was done using Clarity<sup>TM</sup> Western ECL Substrate (Biorad, Hercules, CA, USA). Densitometric analysis was performed using Quantity One Software (Biorad).

## Immunofluorescence

CAF were treated with NT157 with or without IGF-1 for 24 hrs. Then cells were fixed with 4%PFA, permeabilized with 0.01% Triton X-100 and blocked in 2%BSA/1%serum, followed by overnight incubation with GP38 (eBioscience), vimentin (Cell signaling) and  $\alpha$ SMA (Abcam, Cambridge, UK) antibodies. Secondary fluorescent antibodies were added for 1 hr. DAPI was used for nuclear counterstaining. Samples were imaged through a SP5 confocal microscope (Leica Microsystems, Buffalo Grove, IL, USA) 24 hrs after mounting.

## ELISA

Conditioned medium (CM) was collected from BMDM and analyzed using an IL-6 and TNF ELISA kit from eBioscience (San Diego, CA, USA) according to manufacturer's instructions. IGF-1 concentration was determined in serum or CM from tissue explants by an ELISA kit from Abcam. IGF-1 amounts in tissues were normalized to tissue weight and expressed as pg/ml per mg.

## Flow cytometry

Flow cytometric analysis of immune cell populations and CAF was performed by labelling fluorescent cells with tagged antibodies against: CD45, CD4, CD8, CD19, NK1.1, CD11b, F4/80, Gr1, CD11c, MCH-II, EpCam, GP38 (eBioscience), CD31 (BD, Franklin Lakes, NJ, USA), and  $\alpha$ -SMA (Abcam). CAF were determined as CD45<sup>-</sup>EpCAM<sup>-</sup>CD31<sup>-</sup>GP38<sup>+</sup> $\alpha$ SMA<sup>+</sup> cells. Intracellular staining for ROR $\gamma$ t and IL-17A, was performed on MLN and spleen single cell suspensions. Samples were analyzed on a Beckman Coulter Cyan ADP flow cytometer (Beckman Coulter, Indianapolis IN, USA), and data were analyzed with FlowJo.

## Histology

Paraffin-embedded or frozen tissues were stained with H&E, Sirius red, or processed for IHC. Antigens were retrieved with preheated 1xCitrate buffer and were detected by staining with Ki-67 (Genetex, Irvine, CA, USA), cleaved-caspase 3, phosphorylated-STAT3, IGF-1R (Cell Signaling), COX-2, IRS1, PCNA (Santa Cruz), CD11b, GP38 (eBioscience),  $\alpha$ -SMA (Abcam), F4/80 (Caltag, San Mateo, CA, USA) antibodies. The fraction occupied by the positively stained areas was calculated from more than 6 high magnification field (HMF) images per group using ImageJ software.

## RNA Isolation and Real-Time PCR

Total RNA was extracted and mRNA expression was determined as described<sup>13</sup>. The data are presented in arbitrary units and were calculated by  $2^{-(\Delta\Delta CT)}$  method. Primer sequences are listed in Table 1 and were obtained from the NIH qPrimerDepot (<http://mouseprimerdepot.nci.nih.gov>).

## Migration assay

Motility was measured in a modified Boyden chamber using polycarbonate filters (8 $\mu$ m). Cell suspensions were left to attach into the upper chamber for 2 hrs. Cells in the presence or absence of NT157 were left to migrate for 6 hrs after adding IGF-1 alone or with NT157

into the lower compartment. The membranes were stained using Crystal Violet and the transmigrated cells on the lower surface were counted.

### Wound healing assay

Cells were plated and left to grow until confluent. After wounding with a pipette tip, cells were treated with NT157 and/or IGF-1 for 24 hrs. Images were taken at 0 and 24 hrs, and wound size was determined as distance between the edges in pixels.

### Statistical analysis

Results are expressed as averages $\pm$ s.e.m or  $\pm$ s.d. Data were analyzed by Student t-test using GraphPad Prism software. p values $<$  0.05 were considered statistically significant.

### Supplementary Material

Refer to Web version on PubMed Central for supplementary material.

### Acknowledgments

E.S.L was supported by Sara Borrell fellowship ISCIII/MICINN program. S.S. and Z.Z. are CRI Irvington postdoctoral fellows. K.T. is Uehara Memorial Foundation Fellow. Research was supported by NIH grants (AI043477 and CA118165) to MK, who is an American Cancer Society Research Professor and holds the Ben and Wanda Hildyard Chair for Mitochondrial and Metabolic Diseases.

### References

- Schluskel AT, Gagliano RA Jr, Seto-Donlon S, Eggerding F, Donlon T, Berenberg J, et al. The evolution of colorectal cancer genetics-Part 1: from discovery to practice. *J Gastrointest Oncol*. 2014; 5(5):326–335. [PubMed: 25276405]
- Vogelstein B, Kinzler KW. Cancer genes and the pathways they control. *Nat Med*. 2004; 10(8):789–799. [PubMed: 15286780]
- Terzic J, Grivennikov S, Karin E, Karin M. Inflammation and colon cancer. *Gastroenterology*. 2010; 138(6):2101–2114. e2105. [PubMed: 20420949]
- Greten FR, Eckmann L, Greten TF, Park JM, Li ZW, Egan LJ, et al. IKK $\beta$  links inflammation and tumorigenesis in a mouse model of colitis-associated cancer. *Cell*. 2004; 118(3):285–296. [PubMed: 15294155]
- Grivennikov S, Karin E, Terzic J, Mucida D, Yu GY, Vallabhapurapu S, et al. IL-6 and Stat3 are required for survival of intestinal epithelial cells and development of colitis-associated cancer. *Cancer Cell*. 2009; 15(2):103–113. [PubMed: 19185845]
- Grivennikov SI, Karin M. Inflammatory cytokines in cancer: tumour necrosis factor and interleukin 6 take the stage. *Ann Rheum Dis*. 2011; 70(Suppl 1):i104–108. [PubMed: 21339211]
- Putoczki TL1, Thiem S, Loving A, Busuttill RA, Wilson NJ, Ziegler PK, et al. Interleukin-11 is the dominant IL-6 family cytokine during gastrointestinal tumorigenesis and can be targeted therapeutically. *Cancer Cell*. 2013; 24(2):257–271. [PubMed: 23948300]
- Calon A1, Espinet E, Palomo-Ponce S, Tauriello DV, Iglesias M, Céspedes MV, et al. Dependency of colorectal cancer on a TGF- $\beta$ -driven program in stromal cells for metastasis initiation. *Cancer Cell*. 2012; 22(5):571–584. [PubMed: 23153532]
- Lee KW, Yeo SY, Sung CO, Kim SH. Twist1 is a key regulator of cancer-associated fibroblasts. *Cancer Res*. 2015; 75(1):73–85. [PubMed: 25368021]
- Grivennikov SI, Greten FR, Karin M. Immunity, inflammation, and cancer. *Cell*. 2010; 140(6):883–899. [PubMed: 20303878]

11. Mantovani A, Allavena P, Sica A, Balkwill F. Cancer-related inflammation. *Nature*. 2008; 454(7203):436–444. [PubMed: 18650914]
12. Grivennikov SI, Wang K, Mucida D, Stewart CA, Schnabl B, Jauch D, et al. Adenoma-linked barrier defects and microbial products drive IL-23/IL-17-mediated tumour growth. *Nature*. 2012; 491(7423):254–258. [PubMed: 23034650]
13. Wang K, Kim MK, Di Caro G, Wong J, Shalapour S, Wan J, et al. Interleukin-17 receptor a signaling in transformed enterocytes promotes early colorectal tumorigenesis. *Immunity*. 2014; 41(6):1052–1063. [PubMed: 25526314]
14. Joyce JA, Pollard JW. Microenvironmental regulation of metastasis. *Nat Rev Cancer*. 2009; 9(4): 239–252. [PubMed: 19279573]
15. Kalluri R, Zeisberg M. Fibroblasts in cancer. *Nat Rev Cancer*. 2006; 6(5):392–401. [PubMed: 16572188]
16. Straussman R, Morikawa T, Shee K, Barzily-Rokni M, Qian ZR, Du J, Davis A, et al. Tumour micro-environment elicits innate resistance to RAF inhibitors through HGF secretion. *Nature*. 2012; 487(7408):500–504. [PubMed: 22763439]
17. Feng QY, Wei Y, Chen JW, Chang WJ, Ye LC, Zhu DX, et al. Anti-EGFR and anti-VEGF agents: important targeted therapies of colorectal liver metastases. *World J Gastroenterol*. 2014; 20(15): 4263–4275. [PubMed: 24764664]
18. Pollak M. The insulin and insulin-like growth factor receptor family in neoplasia: an update. *Nat Rev Cancer*. 2012; 12(3):159–169. [PubMed: 22337149]
19. Ryan PD, Goss PE. The emerging role of the insulin-like growth factor pathway as a therapeutic target in cancer. *Oncologist*. 2008; 13(1):16–24. [PubMed: 18245009]
20. Surmacz E. Growth factor receptors as therapeutic targets: strategies to inhibit the insulin-like growth factor I receptor. *Oncogene*. 2003; 22(42):6589–6597. [PubMed: 14528284]
21. Giovannucci E. Insulin, insulin-like growth factors and colon cancer: a review of the evidence. *J Nutr*. 2001; 131(11 Suppl):3109S–3120S. [PubMed: 11694656]
22. Woodson K, Flood A, Green L, Tangrea JA, Hanson J, Cash B, et al. Loss of insulin-like growth factor-II imprinting and the presence of screen-detected colorectal adenomas in women. *J Natl Cancer Inst*. 2004; 96(5):407–410. [PubMed: 14996863]
23. Shiratsuchi I, Akagi Y, Kawahara A, Kinugasa T, Romeo K, Yoshida T, et al. Expression of IGF-1 and IGF-1R and their relation to clinicopathological factors in colorectal cancer. *Anticancer Res*. 2011; 31(7):2541–2545. [PubMed: 21873172]
24. Ollberding NJ, Cheng I, Wilkens LR, Henderson BE, Pollak MN, Kolonel LN, et al. Genetic variants, prediagnostic circulating levels of insulin-like growth factors, insulin, and glucose and the risk of colorectal cancer: the Multiethnic Cohort study. *Cancer Epidemiol Biomarkers Prev*. 2012; 21(5):810–820. [PubMed: 22354904]
25. Lee J, Jain A, Kim P, Lee T, Kuller A, Princen F, et al. Activated cMET and IGF1R-driven PI3K signaling predicts poor survival in colorectal cancers independent of KRAS mutational status. *PLoS One*. 2014; 9(8):e103551. [PubMed: 25090459]
26. Heron-Milhavet L, LeRoith D. Insulin-like growth factor I induces MDM2-dependent degradation of p53 via the p38 MAPK pathway in response to DNA damage. *J Biol Chem*. 2012; 277(18): 15600–15606. [PubMed: 11877395]
27. Peretz S, Jensen R, Baserga R, Glazer PM. ATM-dependent expression of the insulin-like growth factor-I receptor in a pathway regulating radiation response. *Proc Natl Acad Sci U S A*. 2001; 98(4):1676–1681. [PubMed: 11172010]
28. Albanell J, Baselga J. Unraveling resistance to trastuzumab (Herceptin): insulin-like growth factor-I receptor, a new suspect. *J Natl Cancer Inst*. 2001; 93(24):1830–1832. [PubMed: 11752000]
29. Jones HE, Goddard L, Gee JM, Hiscox S, Rubini M, Barrow D, et al. Insulin-like growth factor-I receptor signalling and acquired resistance to gefitinib (ZD1839; Iressa) in human breast and prostate cancer cells. *Endocr Relat Cancer*. 2004; 11(4):793–814. [PubMed: 15613453]
30. Huang F, Xu LA, Khambata-Ford S. Correlation between gene expression of IGF-1R pathway markers and cetuximab benefit in metastatic colorectal cancer. *Clin Cancer Res*. 2012; 18(4): 1156–1166. [PubMed: 22294722]

31. Chan BT, Lee AV. Insulin receptor substrates (IRSs) and breast tumorigenesis. *J Mammary Gland Biol Neoplasia*. 2008; 13(4):415–422. [PubMed: 19030971]
32. Ramocki NM, Wilkins HR, Magness ST, Simmons JG, Scull BP, Lee GH, et al. Insulin receptor substrate-1 deficiency promotes apoptosis in the putative intestinal crypt stem cell region, limits Apcmin/+ tumors, and regulates Sox9. *Endocrinology*. 2008; 149(1):261–267. [PubMed: 17916629]
33. Esposito DL, Aru F, Lattanzio R, Morgano A, Abbondanza M, Malekzadeh R, et al. The insulin receptor substrate 1 (IRS1) in intestinal epithelial differentiation and in colorectal cancer. *PLoS One*. 2012; 7(4):e36190. [PubMed: 22558377]
34. Chang Q, Li Y, White MF, Fletcher JA, Xiao S. Constitutive activation of insulin receptor substrate 1 is a frequent event in human tumors: therapeutic implications. *Cancer Res*. 2002; 62(21):6035–6038. [PubMed: 12414625]
35. Reuveni H, Flashner-Abramson E, Steiner L, Makedonski K, Song R, Shir A, et al. Therapeutic destruction of insulin receptor substrates for cancer treatment. *Cancer Res*. 2013; 73(14):4383–4394. [PubMed: 23651636]
36. Hinoi T, Akyol A, Theisen BK, Ferguson DO, Greenson JK, Williams BO, et al. Mouse model of colonic adenoma-carcinoma progression based on somatic Apc inactivation. *Cancer Res*. 2007; 67(20):9721–9730. [PubMed: 17942902]
37. Rojas A, Liu G, Coleman I, Nelson PS, Zhang M, Dash R, et al. IL-6 promotes prostate tumorigenesis and progression through autocrine cross-activation of IGF-IR. *Oncogene*. 2011; 30(20):2345–2355. [PubMed: 21258401]
38. Zhang W, Zong CS, Hermanto U, Lopez-Bergami P, Ronai Z, Wang LH. RACK1 recruits STAT3 specifically to insulin and insulin-like growth factor 1 receptors for activation, which is important for regulating anchorage-independent growth. *Mol Cell Biol*. 2006; 26(2):413–424. [PubMed: 16382134]
39. Zong CS, Chan J, Levy DE, Horvath C, Sadowski HB, Wang LH. Mechanism of STAT3 activation by insulin-like growth factor I receptor. *J Biol Chem*. 2000; 275(20):15099–15105. [PubMed: 10747872]
40. Xiong H, Du W, Sun TT, Lin YW, Wang JL, Hong J, et al. A positive feedback loop between STAT3 and cyclooxygenase-2 gene may contribute to Helicobacter pylori-associated human gastric tumorigenesis. *Int J Cancer*. 2014; 134(9):2030–2040. [PubMed: 24127267]
41. Tang Z, Yu M, Miller F, Berk RS, Tromp G, Kosir MA, et al. Increased invasion through basement membrane by CXCL7-transfected breast cells. *Am J Surg*. 2008; 196(5):690–696. [PubMed: 18954601]
42. Zhou SL, Dai Z, Zhou ZJ, Chen Q, Wang Z, Xiao YS, et al. CXCL5 contributes to tumor metastasis and recurrence of intrahepatic cholangiocarcinoma by recruiting infiltrative intratumoral neutrophils. *Carcinogenesis*. 2014; 35(3):597–605. [PubMed: 24293410]
43. Prager GW, Poettler M. Angiogenesis in cancer. Basic mechanisms and therapeutic advances. *Hamostaseologie*. 2012; 32(2):105–114. [PubMed: 21837355]
44. Bonapace L, Coissieux MM, Wyckoff J, Mertz KD, Varga Z, Junt T, et al. Cessation of CCL2 inhibition accelerates breast cancer metastasis by promoting angiogenesis. *Nature*. 2014; 515(7525):130–133. [PubMed: 25337873]
45. Soubry A, Il'yasova D, Sedjo R, Wang F, Byers T, Rosen C, et al. Increase in circulating levels of IGF-1 and IGF-1/IGFBP-3 molar ratio over a decade is associated with colorectal adenomatous polyps. *Int J Cancer*. 2012; 131(2):512–517. [PubMed: 21898383]
46. Tosolini M, Kirilovsky A, Mlecnik B, Fredriksen T, Mauger S, Bindea G, et al. Clinical impact of different classes of infiltrating T cytotoxic and helper cells (Th1, th2, treg, th17) in patients with colorectal cancer. *Cancer Res*. 2011; 71(4):1263–1271. [PubMed: 21303976]
47. Sonoshita M, Takaku K, Sasaki N, Sugimoto Y, Ushikubi F, Narumiya S, et al. Acceleration of intestinal polyposis through prostaglandin receptor EP2 in Apc(Delta 716) knockout mice. *Nat Med*. 2001; 7(9):1048–1051. [PubMed: 11533709]
48. Arber N, Eagle CJ, Spicak J, Rácz I, Dite P, Hajer J, et al. Celecoxib for the prevention of colorectal adenomatous polyps. *N Engl J Med*. 2006; 355(9):885–895. [PubMed: 16943401]



49. Qian BZ, Pollard JW. Macrophage diversity enhances tumor progression and metastasis. *Cell*. 2010; 141(1):39–51. [PubMed: 20371344]
50. Maeda S, Hikiba Y, Sakamoto K, Nakagawa H, Hirata Y, Hayakawa Y, et al. Ikappa B kinasebeta/nuclear factor-kappaB activation controls the development of liver metastasis by way of interleukin-6 expression. *Hepatology*. 2009; 50(6):1851–1860. [PubMed: 19821485]

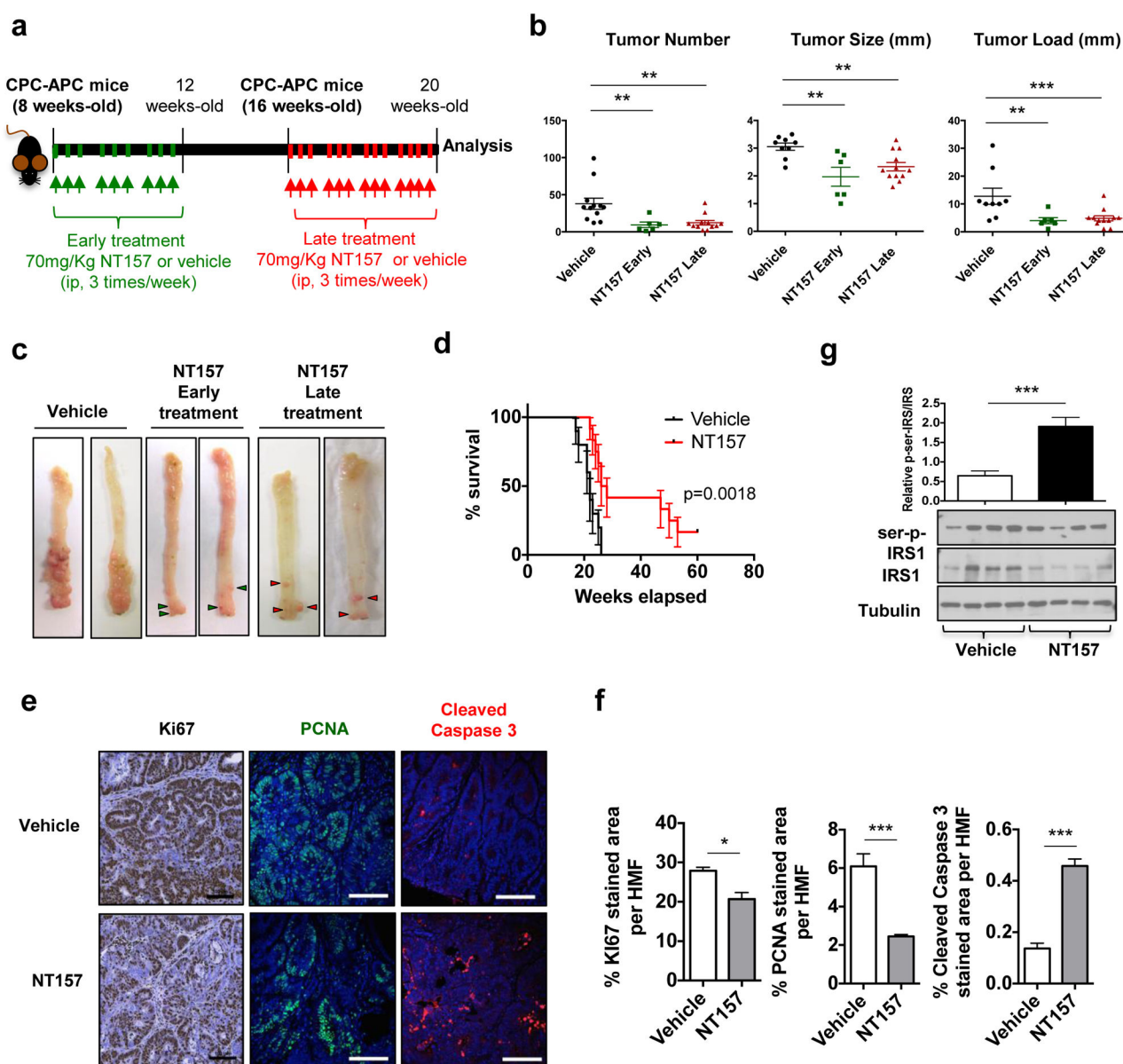


**Figure 1. NT157 treatment reduces colorectal tumor burden**

**a.** CPC-APC mice were i.p. administered 70 mg/Kg NT157 or vehicle (2-hydroxypropyl- $\beta$ -cyclodextrin) 3 times a week, starting at 8 (early) or 16 (late) weeks of age, for 3 or 4 weeks respectively. Animals subjected to early treatment were allowed to develop tumors and tumor burden was analyzed at the same time as in mice subjected to late treatment, i.e. at 20 weeks of age. **b.** Tumor multiplicity, size and load. Results are averages  $\pm$  s.e.m.  $n=6-12$  animals per group.  $**p<0.01$ .  $***p<0.005$ . **c.** Representative images of CPC-APC tumor-bearing colons from treated and untreated mice. **d.** Mice subjected to late treatment were evaluated for survival. Moribund animals were sacrificed and survival was determined by Kaplan-Meier analysis ( $n=10-12$  animals per group) ( $p=0.0018$ ). **e.** Tumor specimens from above mice were subjected to IHC and IF analysis using antibodies to the indicated markers. (scale bars: 100  $\mu$ m). **f.** Fractions (in %) occupied by antibody stained areas are shown as

averages  $\pm$  s.e.m. (n=6–10 HMF per group). \*p<0.05 and \*\*\*p<0.005. **g.** 16 weeks-old CPC-APC mice were treated with NT157 for 4 weeks and sacrificed. Tumors were collected and subjected to immunoblot (IB) analysis with indicated antibodies. The results were quantitated by densitometry, were calculated as p-IRS1/IRS1 and are presented as means  $\pm$  s.e.m. n=8 tumors per group (6–8 animals per group). \*\*\*p<0.005.

Author Manuscript

Author Manuscript

Author Manuscript

Author Manuscript

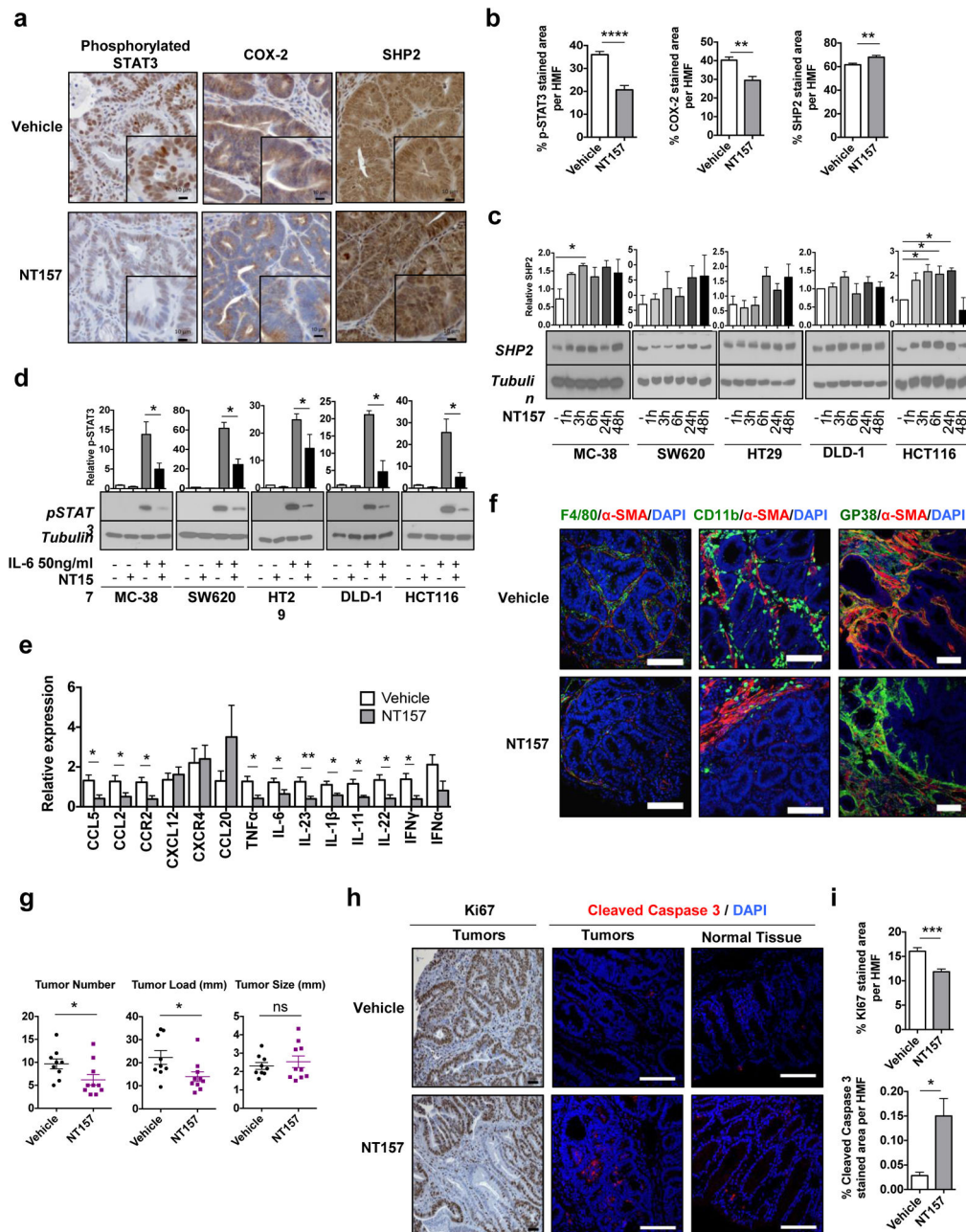


**Figure 2. NT157 treatment reduces tumor associated inflammation and CAF activation**  
CPC-APC mice were subjected to late treatment with NT157 or vehicle as above. Tumors were collected and analyzed. **a.** Tumor sections were analyzed by IHC with indicated antibodies (magnification: 40×, zoomed field scale bars: 10 μm). **b.** Fractions (in %) occupied by antibody stained areas in tumor sections from **a** are shown as averages ± s.e.m. (n= 6–10 HMF of 4–5 animals per group). **c.** MC-38 mouse CRC cells and SW620, HT29, DLD-1 and HCT116 human CRC cell lines were incubated with NT157 (3 μM) for the indicated times. Cell lysates were subjected to IB analysis and quantitated by densitometry. Results are means ± s.e.m (n=2–4 independent experiments). \* p<0.05. **d.** MC-38, SW620,

HT29, DLD-1 and HCT116 cells were incubated with IL-6 (50 ng/ml) for 20 min with or without NT157. Cell lysates were IB analyzed. Results are means  $\pm$  s.e.m (n=2–4 independent experiments). \*  $p<0.05$ . **e.** Expression of cytokine and chemokine mRNAs was determined by Q-PCR in tumors from 20 weeks old mice subjected to late treatment with NT157 or vehicle. Results are means  $\pm$  s.e.m. (n=7–9 mice per group). \*  $p<0.05$ , \*\*  $p<0.01$ . **f.** Frozen tumor sections were subjected to IF analysis with the indicated antibodies. Nuclei were counter stained by DAPI (scale bars: 100  $\mu$ m). **g.** CPC-APC mice (19 weeks old) were given NT157 every other day for a total of 4 times, sacrificed and analyzed 24 hrs after the last injection. Tumor multiplicity, size and load were determined (n=9–10 mice per group). \*  $p<0.05$ . **h.** Paraffin-embedded or frozen tumor and tissue sections were subjected to IHC and IF analyses as above (scale bars 100  $\mu$ m). **i.** Fractions (in %) occupied by antibody stained areas in tumor sections from **h** are shown as averages  $\pm$  s.e.m. (n= 6 to 10 HMF per group). \* $p<0.05$ ; \*\*\* $p<0.005$ .

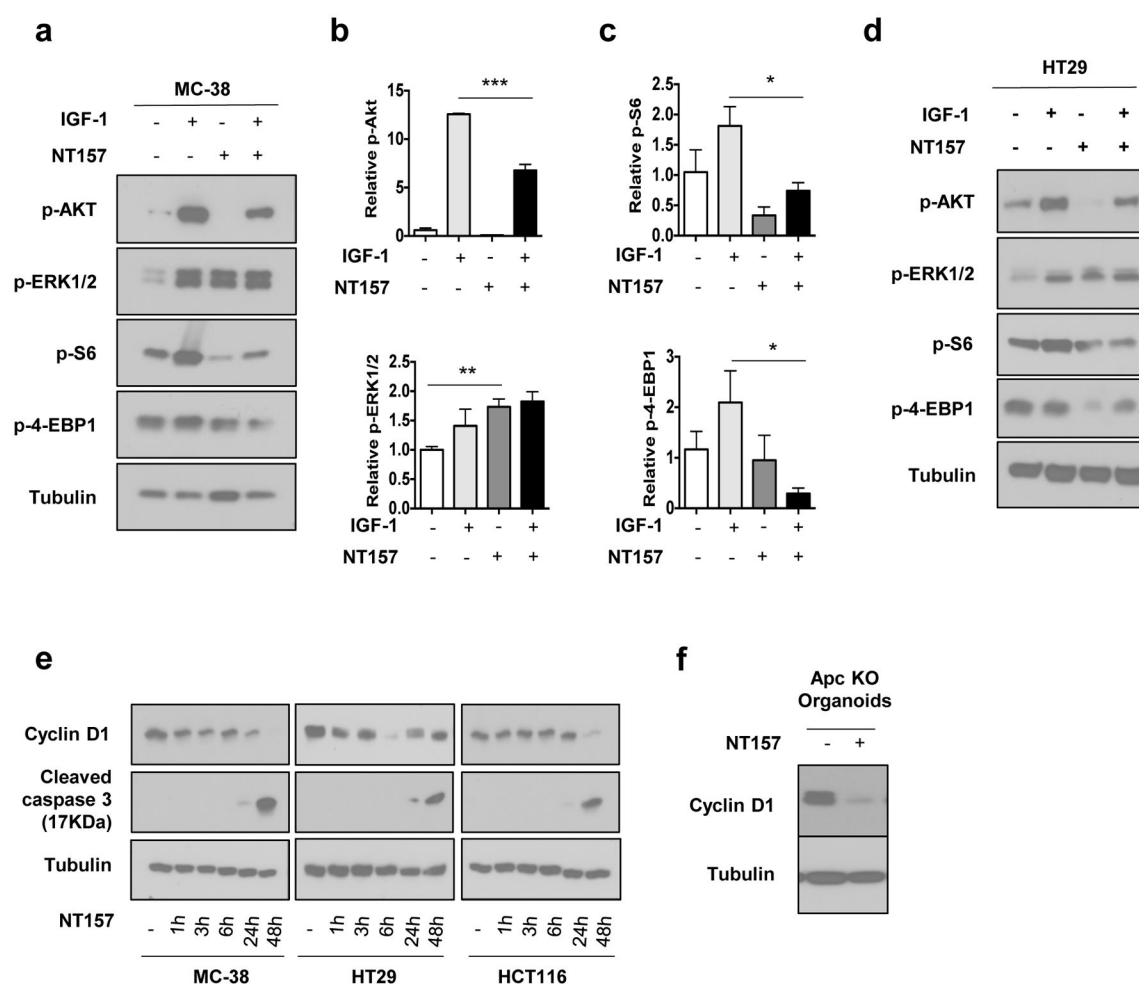


**Figure 3. NT157 inhibits cancer cell proliferation**

**a–c.** MC-38 cells were treated with IGF-1 (100 ng/ml) with or without NT157 (3  $\mu$ M). After 24 hrs, phosphorylation of the indicated proteins was examined by IB analysis and quantitated by densitometry. Results are shown as means  $\pm$  s.e.m.; n=3. \* p<0.05, \*\*\* p<0.005 vs. IGF-1 stimulated cells. **d.** HT29 cells were treated with IGF-1 (100 ng/ml) with or without NT157. After 24 hrs, phosphorylation of the indicated proteins was IB analyzed. Figure shows representative blots of 2 independent experiments. **e.** Expression of the indicated proteins in MC-38, HT29 and HCT116 cells was IB analyzed at the indicated times after NT157 addition (n=2–3 independent experiments). **f.** APC-deficient intestinal organoids were incubated with or without NT157 for 24 hrs and cyclin D1 expression was IB analyzed.



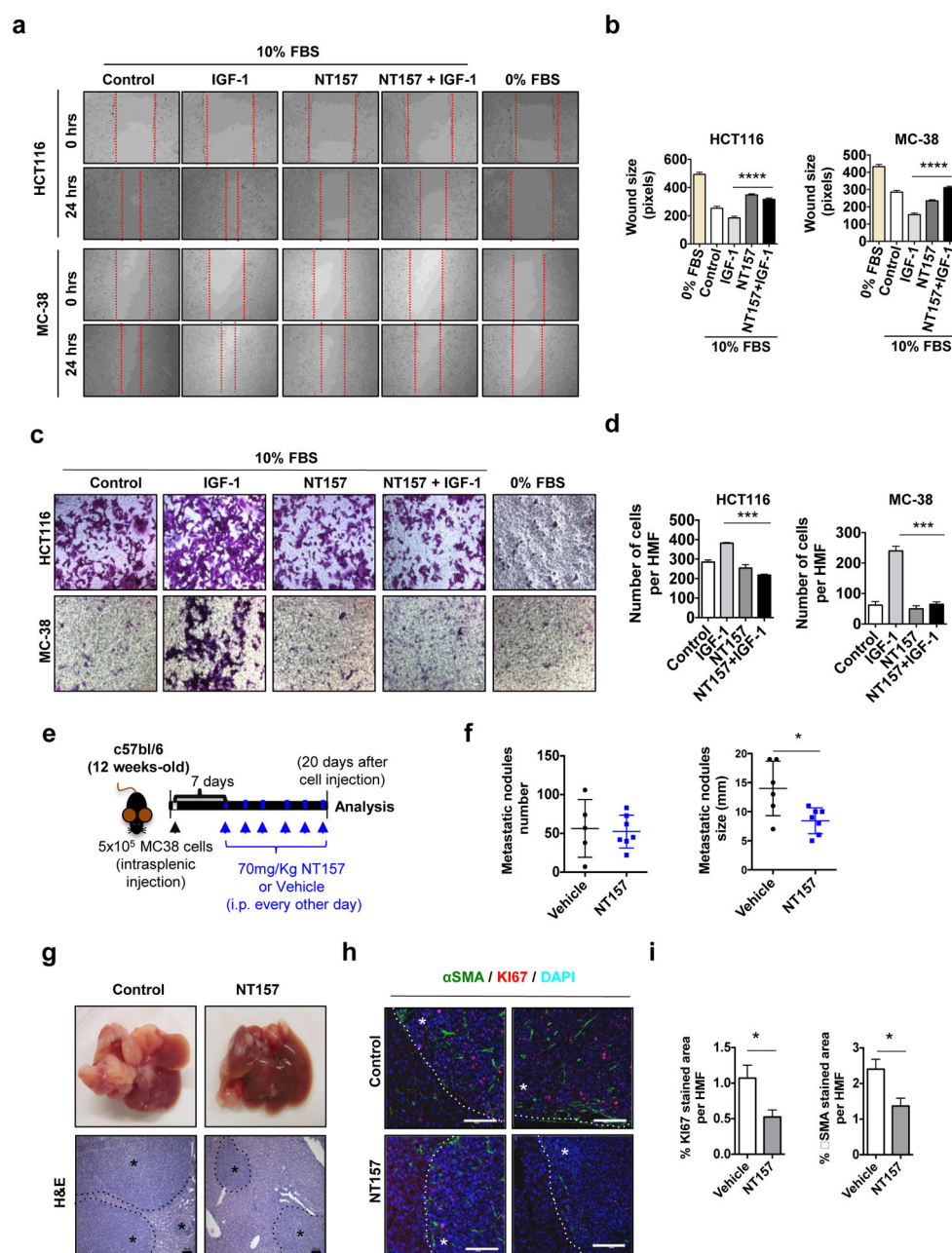


**Figure 4. NT157 treatment decreases the metastatic activity of CRC cells**

**a, b.** HCT116 and MC-38 cells were seeded and grown to confluency. The cell monolayers were scratched and the cells were left to grow in the presence of IGF-1 (100 ng/ml) with or without NT157 (3  $\mu$ M). Images were taken at 0 and 24 hrs, and wound size was determined after 24 hrs using Axo Vision software (distance between the edges in pixels). Three different measurements were recorded from 7–10 fields per condition n=2 independent experiments. \*\*\*\* p<0.001 vs. IGF-1 stimulated cells **c, d.** HCT116 and MC-38 cell migration was determined using Boyden chambers. Briefly,  $2 \times 10^5$  viable cells were seeded on the top compartment and left to attach for 2 hrs, afterwards cells were allowed to migrate

in DMEM supplemented with 10% FBS in the presence or absence of NT157 and after adding IGF-1 to the lower compartment as a chemotactic agent. After 6 hrs, transmigrated cells were stained using crystal violet, photographed and the number of cells per 6 HMF was calculated for each condition. Results are averages  $\pm$  s.e.m. \*\*\*  $p<0.005$ . **e.** MC-38 cells were injected i.s. into C57BL/6 mice. Seven days later the mice were treated with 70 mg/Kg NT157 or vehicle as indicated and sacrificed 20 days after cell inoculation. **f.** Metastatic lesions in liver were enumerated and measured. Results are means  $\pm$  s.e.m. (n=5–7 mice per group). \*  $p<0.05$ . **g.** Representative images of livers from above mice and H&E staining of liver sections (scale bars: 100  $\mu$ m) \* Indicates tumor tissue **h.** Paraffin embedded liver sections were IF analyzed after staining with indicated antibodies (scale bars: 100  $\mu$ m) \* Indicates tumor tissue. **i.** Positively stained areas per each HMF (high magnification field) were quantitated using ImageJ Software. Results are averages  $\pm$  s.e.m. \*  $p<0.05$ . (n=7 HMF per group).

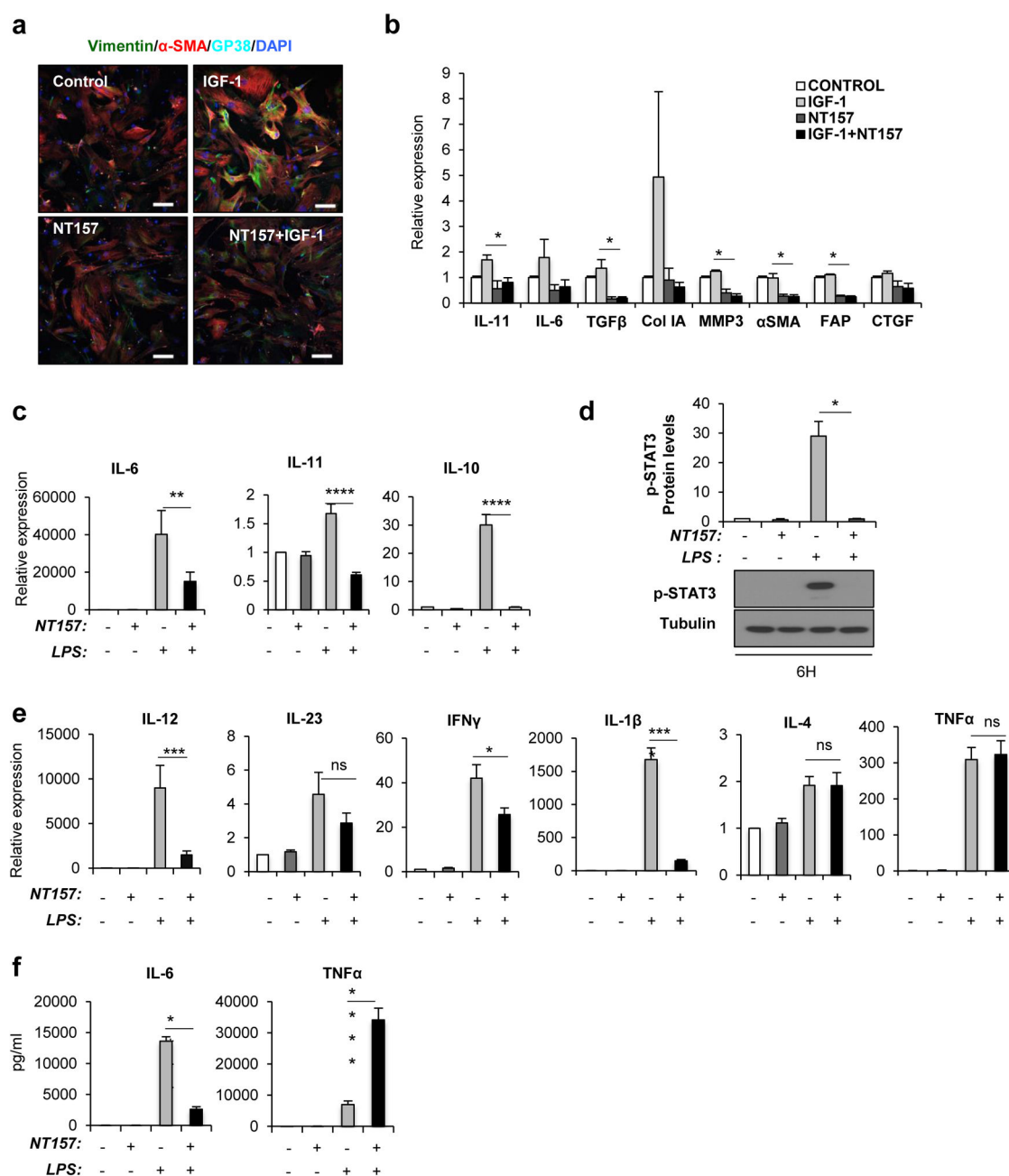


**Figure 5. NT157 prevents CAF and macrophage activation**

**a, b.** CAF were isolated from tumors of 4 months old CPC-APC mice and after expansion in culture, were treated with NT157 (3  $\mu$ M). and/or IGF-1 (100 ng/ml) for 24 hrs. **a.** The cells were stained with indicated antibodies and analyzed by IF microscopy (scale bars: 100  $\mu$ m). **b.** RNA was extracted and expression of indicated mRNAs were quantitated by Q-PCR. Data are means  $\pm$  s.d. (n=3). **c-f.** BMDM isolated from tumor-bearing mice were cultured and treated with or without LPS (1  $\mu$ g/ml) with or without NT157 (3  $\mu$ M), as indicated. **c, e.** Cytokine mRNA expression was examined by Q-PCR. Data are means  $\pm$  s.e.m. (n=4). \* p<0.05, \*\* p<0.01, \*\*\* p<0.005, \*\*\*\* p<0.001 vs. LPS stimulated cells. **d.** STAT3

phosphorylation was evaluated by IB analysis (n=4). **f.** Secretion of IL-6 and TNF from BMDM were measured by ELISA. Data are means  $\pm$  s.e.m. (n=4). \*\*\*\*  $p<0.001$  vs. LPS stimulated cells.

Author Manuscript

Author Manuscript

Author Manuscript

Author Manuscript

TABLE 1

Murine sequences of primers used in the qPCR gene-expression analyses.

| Gene Name | Forward primer sequence (5'-3') | Reverse primer sequence (5'-3') |
|-----------|---------------------------------|---------------------------------|
| CTGF      | cagtggagatgccaggaga             | taatttccctccccggttac            |
| αSMA      | gttcagtggctcctctgtca            | actgggacgacatggaaaag            |
| CXCR4     | tggaccgatcagtgtagt              | gggcaggagaagatcctattga          |
| CXCL12    | ccaaactgtgcccttcagat            | atttcgggtcaatgcacact            |
| CXCR1     | ttctgagcttgctgggaac             | gggtccttcgcctgtataaga           |
| CCL20     | aactgggtgaaaaggctgt             | gtccaattccatcccaaaa             |
| CCL22     | ccagaaggagcacctggac             | catgggcagtgcgaaagta             |
| ICAM1     | tggtagacagcatttacctca           | Ggccaccatcctgttctg              |
| IL-8      | tgctcaaggctggccat               | Gacatcgtagctcttgagtgtca         |
| MMP3      | ccaagtctaactctctggaacctg        | Agagatttgccgcaaaagtg            |
| MIP-2γ    | gacagacggcaggagcac              | Tttcaagcacgcctctctc             |
| IGF-1R    | cactgcatgacgtctctcc             | Gagaatttcctcacaattccatc         |
| IRS1      | ctatgccagcatcagcttcc            | Ttgctgaggtcatttaggtcttc         |
| IRS2      | tgactataccgagatggccttt          | Gaggtgccacgataggtgt             |
| TGFβ      | tggagcaacatgtggaactc            | gtcagcagccggttacca              |
| FAP       | cgcgtaaacacaggattcact           | tcggaggagagttccaatg             |
| Col 1A    | cccctgggtcaagatggtc             | ctccagcctttccaggttct            |
| ICAM1     | tggtagacagcatttacctca           | Ggccaccatcctgttctg              |
| IL-17A    | cagggagagcttcatctgtgt           | Gctgagctttgaggatgat             |
| IL-17F    | ttgatgcagcctgagtgct             | ttgatgcagcctgagtgct             |
| IL-21     | gacattcatcattgacctgtg           | Tcacaggaaggcatttagc             |
| IL-23R    | ccaagtatatgtgcatgtgaaga         | agcttgaggcaagatattgtgt          |
| RORγt     | acctcttttcacgggagga             | tccacatctccacattg               |
| CXCL7     | gccacttcataacctccag             | Gggtccatgccatcagatt             |
| CXCL5     | tagagcccaatctccacac             | Gagctggaggtcattgtg              |
| CCL2      | catccacgtgttggtca               | Gatcatcttgctggatgaatgagt        |
| CCL5      | tgacagagactctgagacagc           | Gagtggtgtccgagccata             |
| IL-11     | gatgtctacctccggcat              | Tcaagagctgtaaacggcg             |
| IL-6      | ccaggtagctatgtactcca            | gctaccaactggctataatc            |
| CCR2      | ggagaaaaagccaactcctca           | Cacagatctctgcctttttgc           |
| TNFα      | cctcacactcagatcatctt            | gctacgacgtgggtacag              |
| IL-1β     | gcaactgttcctgaactcaact          | Atctttgggtccgtcaact             |
| IL-23     | tcctactaggactcagccaac           | Tgggcatctgttggtct               |
| IL-22     | tgacaccagaacatccaga             | aatcgcttgatctctccac             |
| IFNγ      | atctggaggaaactggcaaaa           | Ttcaagactcaagagtctgaggtga       |
| IFNα      | accagcagatcctgaacat             | Aatgagtctaggaggtgttatcc         |
| IL-4      | catcggcattttgaacgag             | Cgagctcactctctgtggtg            |

| Gene Name | Forward primer sequence (5'-3') | Reverse primer sequence (5'-3') |
|-----------|---------------------------------|---------------------------------|
| IL-10     | cagagccacatgctcctaga            | Gtccagctggtcctttgttt            |
| IL-12     | tggtttgccatcgtttgctg            | Acaggtgaggttcactgtttct          |
| RPL32     | gctgccatctgtttacgg              | Tgactggcgctgatgaact             |
| GAPDH     | agcttgatcatcaacgggaag           | Tttgatgttagtggggtctcg           |